Reentrant Superconductivity in $Nb/Cu_{1-x}Ni_x$ Bilayers

V. Zdravkov,[1] A. Sidorenko,[1] G. Obermeier,[2] S. Gsell,[2] M. Schreck,[2] C. Müller,[2] S. Horn,[2] R. Tidecks,[2] and L. R. Tagirov[3]

[1]*Institute of Applied Physics, LISES ASM, Kishinev 2028, Moldova*
[2]*Institut für Physik, Universität Augsburg, D-86159 Augsburg, Germany*
[3]*Solid State Physics Department, Kazan State University, 420008 Kazan, Russia*

(Received 11 February 2006; published 2 August 2006)

We report on the first observation of a pronounced reentrant superconductivity phenomenon in a superconductor/ferromagnet layered system. The results were obtained using a superconductor/ferromagnetic-alloy bilayer of $Nb/Cu_{1-x}Ni_x$. The superconducting transition temperature T_c drops sharply with increasing thickness d_{CuNi} of the ferromagnetic layer, until complete suppression of superconductivity is observed at $d_{CuNi} \approx 4$ nm. Increasing the $Cu_{1-x}Ni_x$ layer thickness further, superconductivity reappears at $d_{CuNi} \geq 13$ nm. Our experiments give evidence for the pairing function oscillations associated with a realization of the quasi-one-dimensional Fulde-Ferrell-Larkin-Ovchinnikov-like state in the ferromagnetic layer.

DOI: 10.1103/PhysRevLett.97.057004 PACS numbers: 74.45.+c, 74.62.−c, 74.78.Db

The coexistence of superconductivity (S) and ferromagnetism (F) in a homogeneous material, described by Fulde-Ferrell and Larkin-Ovchinnikov (FFLO) [1,2], is restricted to an extremely narrow range of parameters [3]. So far, no indisputable experimental evidence for the FFLO state exists.

In general, singlet superconductivity and ferromagnetism do not coexist, since superconductivity requires the conduction electrons to form Cooper pairs with antiparallel spins, whereas ferromagnetism forces the electrons to align their spins parallel. This antagonism can be overcome if superconducting and ferromagnetic regions are spatially separated, as, for example, in artificially layered superconducting/ferromagnetic (S/F) nanostructures (see, e.g., [4] for an early review). The two long-range ordered states influence each other via the penetration of electrons through their common interface. Superconductivity in such a proximity system can survive, even if the exchange splitting energy $E_{ex} \sim k_B \Theta_{Curie}$ in the ferromagnetic layer is orders of magnitude larger than the superconducting order parameter $\Delta \sim k_B T_c$, with T_c the superconducting transition temperature. Cooper pairs entering from the superconducting into the ferromagnetic region experience conditions drastically different from those in a nonmagnetic metal. This is due to the fact that spin-up and spin-down partners in a Cooper pair occupy different exchange-split spin subbands of the conduction band in the ferromagnet. Thus, the spin-up and spin-down wave vectors of electrons in a pair, which have opposite directions, can no longer be of equal magnitude, and the Cooper pair acquires a finite pairing momentum [5]. This results in a pairing function that does not simply decay as in a nonmagnetic metal but, in addition, oscillates on a characteristic length scale. This length scale is the magnetic coherence length ξ_F, which will be specified below.

Various unusual phenomena follow from the oscillation of the pairing wave function in ferromagnets (see, e.g., the recent reviews [6–8] and references therein). A prominent example is the oscillatory S/F proximity effect [9,10]. It can be qualitatively described using the analogy with the interference of reflected light in a Fabry-Pérot interferometer at normal incidence. As the conditions change periodically between constructive and destructive interference upon changing the thickness of the interferometer, the flux of light through the interface of incidence is modulated. In a layered S/F system, the pairing function flux is periodically modulated as a function of the ferromagnetic layer thickness d_F due to the interference. As a result, the coupling between the S and F layers is modulated, and T_c oscillates as a function of d_F.

The most spectacular evidence for the oscillatory proximity effect would be the detection of the reentrant behavior of the superconducting transition temperature as a function of d_F which has been predicted theoretically [11–13]. There is a sole report on the superconductivity reentrance as a function of the ferromagnetic layer thickness in Fe/V/Fe trilayers [14]. Because of the very small thickness of the iron layers at which the reentrance phenomenon is expected (0.7–1.0 nm, i.e., 2–4 monolayers of iron only), the number of the experimental points $T_c(d_F)$ is very small, with a large scattering of the results.

The oscillation length $\xi_{FO} = \hbar v_F / E_{ex}$ in strong ferromagnets, such as iron, nickel, or cobalt, is extremely short, because the exchange splitting energy E_{ex} of the conduction band is in the range 0.1–1.0 eV [4]. Here v_F is the Fermi velocity in the F material and $\hbar$ Planck's constant. Ferromagnetic alloys, with E_{ex} an order of magnitude smaller, allow the observation of the effect at larger layer thicknesses d_F of about 5–10 nm. Such layers can be more easily controlled and characterized. Another advantage of using ferromagnetic alloys is that for a long-wavelength oscillation the atomic-scale interface roughness has no longer a decisive influence on the extinction of the T_c oscillations.

The S/F proximity effect has been studied using not only elemental ferromagnetic materials but also for various ferromagnetic alloys [15–25]. A nonmonotonic dependence of T_c vs d_F has been observed. In the present work, Nb was chosen as the superconductor and a $Cu_{1-x}Ni_x$ alloy, with $x \approx 0.59$ for the ferromagnetic layer. In this alloy, the magnetic momentum and Curie temperature show an almost linear dependence on the Ni concentration [26]. For $x \approx 0.59$, we find $\Theta_{\mathrm{Curie}} \approx 170$ K for bulk material.

The samples were prepared by magnetron sputtering on commercial (111) silicon substrates at 300 K. The base pressure in the "Leybold Z400" vacuum system was about 2×10^{-6} mbar; pure argon (99.999%, "Messer Griesheim") at a pressure of 8×10^{-3} mbar was used as the sputter gas. Three targets, Si, Nb, and $Cu_{40}Ni_{60}$ (75 mm in diameter), were presputtered for 10–15 min to remove contaminations from the targets, as well as to reduce the residual gas pressure of the chamber during the presputtering of Nb, which acts as a getter material. Then we first deposited a silicon buffer layer, using a rf magnetron, to generate a clean interface for the subsequently deposited niobium layer. To deposit high-quality, flat Nb layers with the desired thickness in the range 5–9 nm, we used a motorized, single sweep movement of the target (rotation around the symmetry axis of the chamber) during the dc sputtering process. The average growth rate of the Nb film was about 1.3 nm/sec, while the deposition rate for a fixed, nonmoving target would be about 4 nm/sec. The $Cu_{1-x}Ni_x$ target [27] was rf sputtered (rate 3 nm/sec), resulting in practically the same composition of the alloy in the film. As in our previous work [28], we deposited a wedge-shaped ferromagnetic layer to obtain a series of samples with varying ferromagnetic $Cu_{1-x}Ni_x$ layer thickness. To prepare this wedge, the 80 mm long and 7 mm wide silicon substrate was mounted at a distance of 4.5 cm from the $Cu_{1-x}Ni_x$ target symmetry axis to utilize the intrinsic spatial gradient of the deposition rate. To prevent the degradation of the $Nb/Cu_{1-x}Ni_x$ bilayers at atmospheric conditions, the bilayers were coated by a silicon layer of about 5 nm thickness. A sketch of the resulting wedgelike samples is presented in the inset in Fig. 1. Samples of equal width were cut across the wedge, to obtain a set of 2.5 mm wide strips with varying $Cu_{1-x}Ni_x$ layer thickness. Aluminum wires 50 μm in diameter were then attached to the strips by ultrasonic bonding for four-probe resistance measurements. Two batches of samples were prepared: one with $d_{\mathrm{Nb}} \approx 7.3$ nm (S15), the other with $d_{\mathrm{Nb}} \approx 8.3$ nm (S16).

After investigating the transition into the superconducting state by measuring resistance-temperature $R(T)$ curves, Rutherford backscattering spectrometry (RBS) has been used to evaluate the thickness of the Nb and $Cu_{1-x}Ni_x$ layers as well as to check the concentration of Cu and Ni in the deposited alloy layers (Fig. 1). The applicability of this

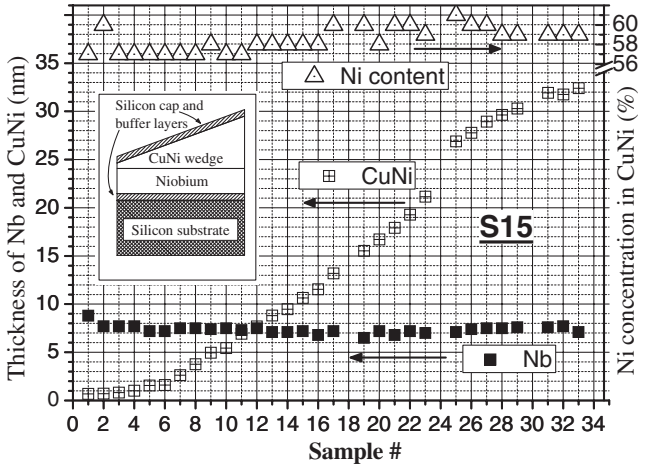

FIG. 1. Results of a RBS investigation: S15 batch of samples, $d_{\mathrm{Nb}} \approx 7.3$ nm. The RBS error bars are within the point size.

method for thickness determination has been demonstrated in our previous work [28]. It allows determining the thickness (via the areal density) of the layers with an accuracy of $\pm 3\%$ for $Cu_{1-x}Ni_x$ on the thick side of the $Cu_{1-x}Ni_x$ wedge and $\pm 5\%$ for Nb and $Cu_{1-x}Ni_x$ on the thin side of the wedge. The measurements were performed with 3.5 MeV He^{++} ions delivered by a tandem accelerator. The backscattered ions were detected under an angle of 170° with respect to the incident beam by a semiconductor detector. In order to avoid channeling effects in the Si substrate, the samples were tilted by 7° and azimuthally rotated during the measurement. The spectra were simulated using the RUMP computer program [29]. From the deduced elemental areal densities of Nb and $Cu_{1-x}Ni_x$ alloy, the thickness of the two layers was calculated using the densities of the respective metals. The results for the layer thickness and $Cu_{1-x}Ni_x$ alloy composition as a function of position on the substrate of batch S15 are shown in Fig. 1. The Ni concentration in the $Cu_{1-x}Ni_x$ layer is nearly constant, showing a slight increase towards the thick side of the wedge. The thickness of the Nb layer is nearly constant along the wedge, $d_{\mathrm{Nb}}(\mathrm{S15}) \approx 7.3$ nm.

The resistance measurements were performed in a ^{3}He cryostat and a dilution refrigerator. The standard dc four-probe method was used, applying a sensing current of 10 μA in the temperature range 0.4–10 K and of 2 μA for 40 mK–1.0 K, respectively. The polarity of the current was alternated during the resistance measurements to eliminate possible thermoelectric voltages. The superconducting critical temperature T_c was determined from the midpoints of the $R(T)$ curves at the superconducting transition (Fig. 2). The transition width (defined by the temperature interval in which the resistance changes from $0.1R_n$ to $0.9R_n$, with R_n the normal state resistance just above the transition) was below 0.2 K for most of the investigated samples. The shift between transitions mea-

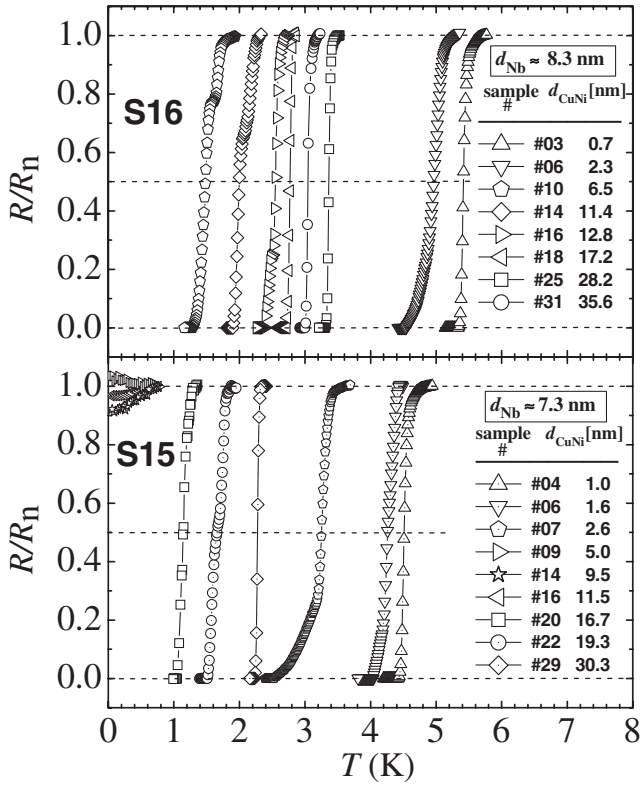

FIG. 2. Typical resistive transitions of the investigated samples. The solid lines are a guide to the eye.

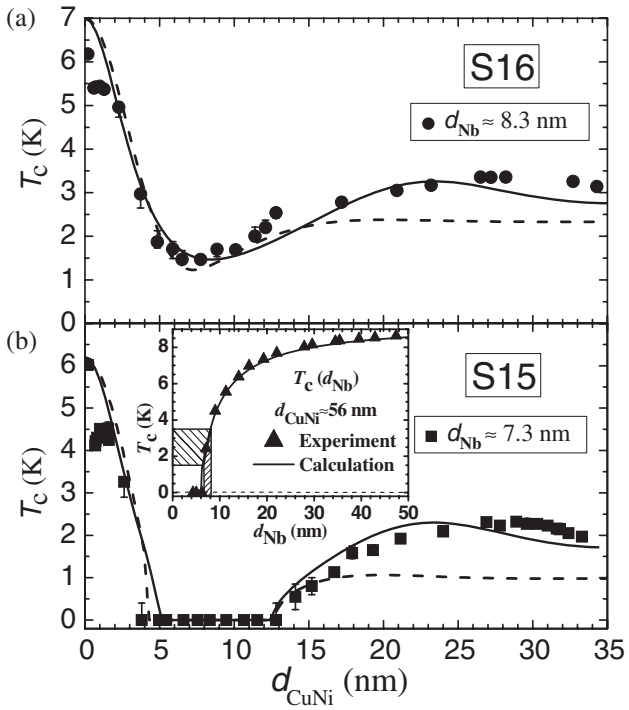

FIG. 3. Nonmonotonous $T_c(d_F)$ dependence for Nb/$Cu_{41}Ni_{59}$ bilayers: (a) $d_{Nb} \approx 8.3$ nm; (b) $d_{Nb} \approx 7.3$ nm. Transition widths are within the point size if error bars are not visible. The solid and dashed lines are theoretical curves for the clean and dirty cases, respectively (see the text). The inset shows $T_c(d_{Nb})$ for a $Cu_{41}Ni_{59}$ top layer of constant thickness with the solid line calculated for the clean case. The calculated critical thickness ($T_c \to 0$ K) is $d_{Nb}^{cr} \approx 6.2$ nm.

sured for increasing and decreasing temperature was smaller than 15 mK.

Figure 3 demonstrates for two values of the Nb layer thickness [$d_{Nb} \approx 8.3$ nm in Fig. 3(a) and $d_{Nb} \approx 7.3$ nm in Fig. 3(b)] the dependence of the superconducting transition temperature on the thickness of the $Cu_{41}Ni_{59}$ layer. For specimens with $d_{Nb} \approx 8.3$ nm, the transition temperature T_c reveals a nonmonotonic behavior with a deep minimum at about $d_{CuNi} \approx 7.0$ nm. For $d_{Nb} \approx 7.3$ nm, the transition temperature decreases sharply upon increasing the ferromagnetic $Cu_{41}Ni_{59}$ layer thickness, until $d_{CuNi} \approx 3.8$ nm. Then, in the range $d_{CuNi} \approx 4.0$–12.5 nm, the superconducting transition temperature vanishes (at least, T_c is lower than the lowest temperature measured in our cryogenic setup, i.e., 40 mK). For $d_{CuNi} > 12.5$ nm, a superconducting transition is observed again with T_c increasing up to about 2 K. This phenomenon of reentrant superconductivity in the superconductor-ferromagnetic-alloy system is the most important finding of the study presented here.

For the regions of values of d_{CuNi} for which T_c changes rapidly, the transition width is wider than 0.2 K and the $R(T)$ curve appears slightly asymmetric with respect to the midpoint of the transition. This is probably due to the small variation of the thickness of the ferromagnetic layer within each sample, since they were cut from a wedge as described above.

For a comparison with the theory, we first tried to fit our data with the formulas of Ref. [12] for the "dirty" case (e.g., of an alloy with electronic mean free path $l_F \ll \xi_{FO}$) taking into account the "2/5" correction factor in the diffusion coefficient of the ferromagnetic alloy according to Refs. [30,31]. The curves were calculated with the following parameters: the superconducting coherence length $\xi_S = 10.2$ nm, the ratio of the Sharvin conductances $N_F\nu_F/N_S\nu_S = 0.25$, the S/F-interface transparency parameter $T_F = 0.845$, $l_F/\xi_{FO} = 0.5$, and $\xi_{FO} = 13.8$ nm. The BCS coherence length for Nb was taken $\xi_{BCS} = 42$ nm [32]. However, we failed to reproduce T_c of the reentrant region for the S15 batch and the amplitude of $T_c(d_{CuNi})$ variations for batch S16 (Fig. 3, dashed curves). The multimode approach [33,34] did not improve compliance with the experiment.

Next we used the formulas adapted to the case of a "clean" ferromagnet ($l_F \gg \xi_{FO}$) as described in Ref. [12] and elaborated for a practical use in Ref. [28]. The resulting solid curves in Fig. 3 are calculated with the following parameters: $\xi_S = 10.2$ nm (S15), $\xi_S = 10.5$ nm (S16). Moreover, $N_F\nu_F/N_S\nu_S = 0.17$, $T_F = 0.845$, $l_F/\xi_{FO} = 1.2$, and $\xi_{FO} = 8.6$ nm.

The inset in Fig. 3 shows $T_c(d_{\mathrm{Nb}})$ for a "thick" $Cu_{41}Ni_{59}$ top layer ($d_{\mathrm{CuNi}} \approx 56$ nm) together with the theory using the parameters for batch S15 given above. The shadowed area indicates the asymptotic values of $T_c(d_{\mathrm{CuNi}} \rightarrow \infty)$ for Nb films of 6.5–8.5 nm thickness. This region of steep T_c variation is the key condition to observe large-amplitude oscillations of the superconducting T_c.

The solid curves of $T_c(d_{\mathrm{CuNi}})$ in Fig. 3 agree best with the measured values. The electron mean free path $l_F \approx 10.3$ nm, used in our calculations, appeared to be longer than the coherence length $\xi_{FO} = 8.6$ nm. Thus, our $Cu_{41}Ni_{59}$ alloy is between the dirty and the clean cases. According to Ref. [21], $l_F \approx 4.4$ nm for a $Cu_{47}Ni_{53}$ alloy with resistivity $\rho_F = 57\ \mu\Omega\,\mathrm{cm}$ (bulk material, $T = 10$ K). Assuming that the product $\langle \rho_F l_F \rangle \approx 2.5 \times 10^{-5}\ \mu\Omega\,\mathrm{cm}^2$ remains unchanged upon adding impurities [35], we get $l_F \sim 10$ nm for our $Cu_{41}Ni_{59}$ alloy using our data for the low-temperature resistivity $\rho_F \approx 25\ \mu\Omega\,\mathrm{cm}$. Thus, both the proximity and the resistivity analysis indicate that our $Cu_{41}Ni_{59}$ alloy is closer to the clean case.

The small cusplike structure in the $T_c(d_{\mathrm{CuNi}})$ dependence at $d_{\mathrm{CuNi}} \approx 1$ nm cannot be explained by any of the theoretical approaches [12,33,34]. We may assume that at $d_{\mathrm{CuNi}} \leq 1$ nm the $Cu_{1-x}Ni_x$ layer is magnetically inhomogeneous. Then enhanced spin-flip scattering of conduction electrons may cause a downturn of the superconducting T_c to smaller thicknesses.

In conclusion, we present the first conclusive experimental observation of the reentrant behavior of superconductivity and large-amplitude oscillations of the superconducting T_c in two series of superconducting/ferromagnetic bilayers with a constant Nb layer thickness ($d_{\mathrm{Nb}} \approx 7.3$ nm and $d_{\mathrm{Nb}} \approx 8.3$ nm) and varied thickness of a $Cu_{41}Ni_{59}$ alloy layer.

The authors are grateful to V. Ryazanov and V. Oboznov for stimulating discussions and cooperation and to Yu. Shalaev for technical assistance in constructing the target-holder movement setup. The work was partially supported by INTAS (Grant No. YSF 03-55-1856) and BMBF (Project No. MDA02/002).

[1] P. Fulde and R. Ferrell, Phys. Rev. **135**, A550 (1964).
[2] A. I. Larkin and Yu. N. Ovchinnikov, Zh. Eksp. Teor. Fiz. **47**, 1136 (1964) [Sov. Phys. JETP **20**, 762 (1965)].
[3] P. Fulde, Adv. Phys. **22**, 667 (1973), Fig. 22.
[4] C. L. Chien and D. H. Reich, J. Magn. Magn. Mater. **200**, 83 (1999).
[5] E. A. Demler, G. B. Arnold, and M. R. Beasley, Phys. Rev. B **55**, 15 174 (1997).
[6] A. A. Golubov, M. Yu. Kupriyanov, and E. Il'ichev, Rev. Mod. Phys. **76**, 411 (2004).
[7] I. F. Lyuksyutov and V. L. Pokrovsky, Adv. Phys. **54**, 67 (2005).
[8] A. I. Buzdin, Rev. Mod. Phys. **77**, 935 (2005).
[9] Z. Radović, M. Ledvij, L. Dobrosavljević-Grujić, A. I. Buzdin, and J. R. Clem, Phys. Rev. B **44**, 759 (1991).
[10] J. S. Jiang, D. Davidović, D. H. Reich, and C. L. Chien, Phys. Rev. Lett. **74**, 314 (1995).
[11] M. G. Khusainov and Yu. N. Proshin, Phys. Rev. B **56**, R14 283 (1997); **62**, 6832(E) (2000).
[12] L. R. Tagirov, Physica (Amsterdam) **307C**, 145 (1998).
[13] B. P. Vodopyanov and L. R. Tagirov, Pis'ma Zh. Eksp. Teor. Fiz. **78**, 1043 (2003) [JETP Lett. **78**, 555 (2003)].
[14] I. A. Garifullin, D. A. Tikhonov, N. N. Garif'yanov, L. Lazar, Yu. V. Goryunov, S. Ya. Khlebnikov, L. R. Tagirov, K. Westerholt, and H. Zabel, Phys. Rev. B **66**, 020505(R) (2002).
[15] L. V. Mercaldo, C. Attanasio, C. Coccorese, L. Maritato, S. L. Prischepa, and M. Salvato, Phys. Rev. B **53**, 14 040 (1996).
[16] M. Schöck, C. Sürgers, and H. v. Löhneysen, Eur. Phys. J. B **14**, 1 (2000).
[17] J. Y. Gu, C.-Y. You, J. S. Jiang, J. Pearson, Ya. B. Bazaliy, and S. D. Bader, Phys. Rev. Lett. **89**, 267001 (2002).
[18] A. Rusanov, R. Boogaard, M. Hesselberth, H. Sellier, and J. Aarts, Physica (Amsterdam) **369C**, 300 (2002).
[19] H. Sellier, C. Baraduc, F. Lefloch, and R. Calemczuk, Phys. Rev. B **68**, 054531 (2003).
[20] V. V. Ryazanov, V. A. Oboznov, A. S. Prokofiev, and S. V. Dubonos, Pis'ma Zh. Eksp. Teor. Fiz. **77**, 43 (2003) [JETP Lett. **77**, 39 (2003)].
[21] A. Potenza and C. H. Marrows, Phys. Rev. B **71**, 180503 (2005).
[22] J. Kim, J. Hyung Kwon, K. Char, H. Doh, and H.-Y. Choi, Phys. Rev. B **72**, 014518 (2005).
[23] L. Crétinon, A. K. Gupta, H. Sellier, F. Lefloch, M. Fauré, A. Buzdin, and H. Courtois, Phys. Rev. B **72**, 024511 (2005).
[24] C. Cirillo, S. L. Prischepa, M. Salvato, C. Attanasio, M. Hesselberth, and J. Aarts, Phys. Rev. B **72**, 144511 (2005).
[25] G. P. Pepe, R. Latempa, L. Parlato, A. Ruotolo, G. Ausanio, G. Peluso, A. Barone, A. A. Golubov, Ya. V. Fominov, and M. Yu. Kupriyanov, Phys. Rev. B **73**, 054506 (2006).
[26] S. V. Vonsovskii, *Magnetism* (Wiley, New York, 1974).
[27] The $Cu_{1-x}Ni_x$ targets were fabricated in the laboratory of Professor V. V. Ryazanov, ISSP of RAS, Chernogolovka.
[28] A. S. Sidorenko, V. I. Zdravkov, A. Prepelitsa, C. Helbig, Y. Luo, S. Gsell, M. Schreck, S. Klimm, S. Horn, L. R. Tagirov, and R. Tidecks, Ann. Phys. (Berlin) **12**, 37 (2003).
[29] L. R. Doolittle, Nucl. Instrum. Methods Phys. Res., Sect. B **9**, 344 (1985).
[30] Ya. V. Fominov, M. Yu. Kupriyanov, and M. V. Feigel'man, Phys. Usp. **46**, 105 (2003).
[31] A. I. Buzdin and I. Baladie, Phys. Rev. B **67**, 184519 (2003).
[32] C. Strunk, C. Sürgers, U. Paschen, and H. v. Löhneysen, Phys. Rev. B **49**, 4053 (1994).
[33] Ya. V. Fominov, N. M. Chtchelkatchev, and A. A. Golubov, Phys. Rev. B **66**, 014507 (2002).
[34] Chun-Yeol You, Ya. B. Bazaliy, J. Y. Gu, S.-J. Oh, L. M. Litvak, and S. D. Bader, Phys. Rev. B **70**, 014505 (2004).
[35] R. A. French, Cryogenics **8**, 301 (1968).